

## THE FIRST DEFINITE DETECTION OF X-RAYS FROM AN EXTREMELY YOUNG PROTOSTAR

K. Hamaguchi<sup>1,2</sup>, M. F. Corcoran<sup>1,2</sup>, R. Petre<sup>1</sup>, N. E. White<sup>1</sup>, B. Stelzer<sup>3</sup>, K. Nedachi<sup>4</sup>, N. Kobayashi<sup>4</sup>, and A. T. Tokunaga<sup>5</sup>

<sup>1</sup>Exploration of the Universe Division, Goddard Space Flight Center, Greenbelt, MD 20771, USA

<sup>2</sup>Universities Space Research Association, 10211 Wincopin Circle, Suite 500, Columbia, MD 21044-3432

<sup>3</sup>INAF, Osservatorio Astronomico di Palermo, Piazza del Parlamento 1, I-90134 Palermo, Italy

<sup>4</sup>Institute of Astronomy, University of Tokyo, 2-21-1 Osawa, Mitaka, Tokyo 181-0015, Japan

<sup>5</sup>Institute for Astronomy, University of Hawaii, 2680 Woodlawn Drive, Honolulu, HI 96822, USA

### ABSTRACT

Class I protostars exhibit powerful X-ray emission. Their X-ray activity can exceed those of older stars such as T-Tauri and main-sequence stars. Without surface convection to drive a solar-type dynamo mechanism, X-ray activity is suspected to be driven by magnetic activity linked to the mass accretion process. Mass accretion is thought to be more intense in the earliest Class 0 protostar phase, but X-ray emission from them has not been conclusively detected so far. This could be due to stronger X-ray absorption to their protostellar cores, or a certain transition in high energy activity between the Class 0 and Class I phases.

With two XMM-Newton observations on March 2003, we detected for the first time strong X-ray emission from an extremely embedded source in the R Corona Australis star forming core, IRS 7 region (Hamaguchi et al., 2005). The source has the radio counterpart 10E (IRS7B) but no near-IR counterpart. These facts plus the strong X-ray absorption of  $N_{\text{H}} \sim 3 \times 10^{23} \text{ cm}^{-2}$  (equivalent to  $A_{\text{V}} \sim 180^m$ ) indicate that the source is a Class 0 or perhaps a Class 0/I protostar. The X-ray spectrum showed thermal emission with  $kT = 3\text{--}4 \text{ keV}$  with the luminosity up to  $10^{31.2} \text{ ergs s}^{-1}$ . The light curve showed gradual flux increase by a factor of two during 30 ksec, unlike solar-type magnetically driven X-ray flares which have smaller variation timescales. The source was 10–100 times fainter during Chandra observations which occurred before and after the XMM-Newton observations. The flux enhancement on month timescales might be driven by sporadic mass accretion episode, while the short-term variation during the XMM-Newton observation could be related to the proto-stellar core rotation.

Key words: young stars; magnetic field; X-rays.

### 1. INTRODUCTION

Low-mass protostars are divided into two classes, Class 0 and Class I, according to their infrared (IR) and radio spectral energy distribution (SED). This classification generally traces their evolutionary status. Class 0 objects are thought to be young ( $t \sim 10^4 \text{ yr}$ ) protostars which mainly emit in the far-IR and submillimeter wavelengths with blackbody temperatures of  $< 30 \text{ K}$  (André et al., 1993). They are believed to be accreting mass dynamically from their huge circumstellar envelopes. Class I objects are believed to be older protostars ( $t \sim 10^5 \text{ yr}$ ) at the end of the mass-accretion phase and emit in the near-IR at temperatures of  $T \sim 3000\text{--}5000 \text{ K}$ .

Protostellar cores are generally hidden inside enormous gas envelopes. Hard X-rays can penetrate the thick molecular clouds, and hard X-ray observations have revealed high energy activity associated with Class I objects (Koyama et al., 1996; Grosso et al., 1997; Imanishi et al., 2001). The observed X-ray emission exhibits occasional rapid outbursts reminiscent of solar flares though current star formation theories do not predict solar-type magnetic dynamos in very young stars. Montmerle et al. (2000) proposed an alternative dynamo mechanism, in which fossil magnetic fields link the protostellar core with its circumstellar disk reconnect.

Hard X-ray emission from other embedded sources was reported in the OMC-2/3 cloud (Tsuboi et al., 2001). The two detected sources show Class 0 characteristics: huge absorption ( $N_{\text{H}} \sim 1 - 3 \times 10^{23} \text{ cm}^{-2}$ ), no near-IR counterparts, and associations with millimeter radio clumps. However, follow-up radio and near-IR observations by Tsujimoto et al. (2004) did not unambiguously classify them as Class 0 protostars. In particular, one of these sources correlates with a centimeter radio source and a jet feature in the  $\text{H}_2$  band, which indicates excitation by a jet from a nearby Class I protostar. Though Skinner et al. (2003) and Rho et al. (2004) have reported X-ray emis-



Figure 1. Left: *XMM-Newton* “true-color” image of the R CrA star forming region. The image is color coded to represent hard band (3–9 keV) to blue, medium band (1–3 keV) to green, and soft band (0.2–1 keV) to red. Right: JHK Infrared image of the R CrA star forming core, taken with the University of Hawaii 88-inch telescope. The bright source at the center is the Herbig Be star, R CrA.

sion from other millimeter radio clumps in NGC 2024 and the Trifid nebula, the photon statistics in those observations were too limited ( $\lesssim 50$  photons per source) to identify their nature conclusively. On the other hand, a survey by Montmerle (2005) has detected X-rays from none of Class 0 protostars. To date no X-ray source has been clearly identified with a bona-fide Class 0 object.

The R Corona Australis (R CrA) cloud is a nearby star forming region ( $d \sim 170$  pc, Knude & Høg, 1998). Among many young stellar objects in the cloud, those in the IRS 7 region have attracted particular interest as a site of ongoing star formation. The region contains double peaked, strong centimeter emission; an eastern peak is designated as 10E or IRS 7B, and a western peak is designated 10W or IRS 7A (Brown, 1987; Feigelson et al., 1998; Harju et al., 2001). It also contains two submillimeter peaks (van den Ancker, 1999), multiple millimeter continuum peaks (Henning et al., 1994; Saraceno et al., 1996; Chini et al., 2003; Choi & Tatematsu, 2004), and a signature of strong bipolar outflows (Harju et al., 1993; Anderson et al., 1997), but only one near-IR source, IRS 7 (Wilking et al., 1997, W97). These characteristics make the IRS 7 region a promising host of Class 0 sources. Koyama et al. (1996) detected hard X-ray emission and an intense flare from the IRS 7 region, which suggested the presence of a magnetically active protostar.

We report the strong X-ray emission of an extremely embedded source in the IRS 7 star forming core in the R Corona Australis cloud, detected during *XMM-Newton* observations on March 28, 2003 (Obs<sub>XMM1</sub>) and March 29, 2003 (Obs<sub>XMM2</sub>) each with a 30 ksec exposure.

## 2. OBSERVATIONS AND RESULTS

### 2.1. Image

Figure 1 left shows an X-ray true-color image of the R Corona Australis Cloud, which combines the data taken in two *XMM-Newton* observations in 2003. In this image, the Herbig Be star TY CrA at the top and Weak-line T-Tauri star CrA 1 at the bottom are seen in white, while Class I protostar candidates at the center are seen in light blue since soft X-rays shown in red is not transparent to the huge circumstellar envelopes of those protostars. These protostars are seen in red in the infrared image at the right panel of Figure 1 because of the infrared extinction.

At the east of those protostars, we found two dark blue sources (Figure 2 for the magnified image). A faint X-ray source at north west is identified as the infrared source IRS7(A), which has been suspected to be younger than Class I protostars. (Wilking et al., 1997). The other bright X-ray source at south east has the radio counterpart source 10E (IRS7B) (Brown, 1987; Feigelson et al., 1998), but it has no *K*-band counterpart with the small upper-limit ( $19.4^m$ , Hamaguchi et al., 2005). Latest infrared observations with VLT and Subaru found an infrared counterpart at  $\lambda \gtrsim 3.8\mu\text{m}$  (Pontoppidan et al., 2003, Nedachi et al. in preparation, see the bottom panel of Figure 2). In sub-millimeter wavelength, van den Ancker (1999) and Nutter et al. (2005) found a strong condensation around IRS7B, whose spectral energy distribution combined with another condensation at the south can be reproduced with the blackbody radiation of 10–15 K. On the other hand, the absorption to the source in X-rays is measured at  $N_{\text{H}} \sim 2.8 \times 10^{23} \text{ cm}^{-2}$  (see section 2.3), equivalent to  $A_{\text{V}} \sim 180^m$  using the  $N_{\text{H}}\text{--}A_{\text{V}}$  relation by

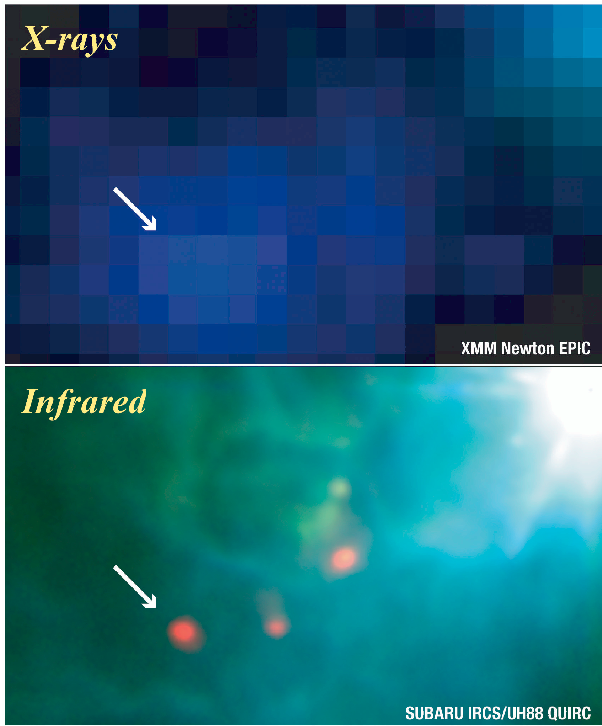


Figure 2. The XMM-Newton image of the IRS 7 star forming core (top) and the HKL infrared image taken with the University of Hawaii 88 inch telescope (HK) and the Subaru telescope (L) (bottom). The arrows show IRS7B. The pink source at the center and the bright source at the top right in the bottom panel are IRS7A and R CrA, respectively.

Imanishi et al. (2001). These results suggest that the X-ray source is extremely embedded in the dark cloud, presumably a Class 0 protostar.

## 2.2. Light Curve

*Chandra* observed the same field  $\sim 2$  years before (2000 October) and 3 months after (2003 June) those XMM-Newton observations. We analyzed the archival data and found an X-ray source at the position of IRS7B, which has  $\sim 20$  photons in each observation for 20–40 ksec. The observed flux,  $1\text{--}3 \times 10^{-14}$  ergs  $\text{cm}^{-2}$   $\text{s}^{-1}$ , was a factor of 10–100 times fainter than the flux during the XMM-Newton observations (Figure 3).

Though the X-ray activity enhanced strongly during the XMM-Newton observations in 2003, the light curves are not like a magnetically-generated X-ray flare. Figure 4 shows the background subtracted EPIC pn+MOS light curve of IRS7B in the 2–10 keV band. The first half of the light curve, corresponding to Obs<sub>XMM1</sub>, is mostly flat with some indications of a slight increase at the end. The source was about four times brighter than the average count rate of Obs<sub>XMM1</sub> at the beginning of the second half, corresponding to Obs<sub>XMM2</sub>, and the count rate gradually increased by a factor of two. This part of the light curve can be acceptably fit at greater than 90% confidence

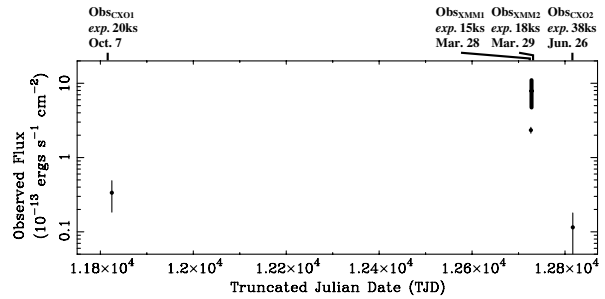


Figure 3. Observed X-ray flux between 0.5–10 keV in long time scale. The vertical narrow bars on the data points show photon statistical error at 90% confidence level. The thick bar shows the variable range of IRS7B during Obs<sub>XMM2</sub>.

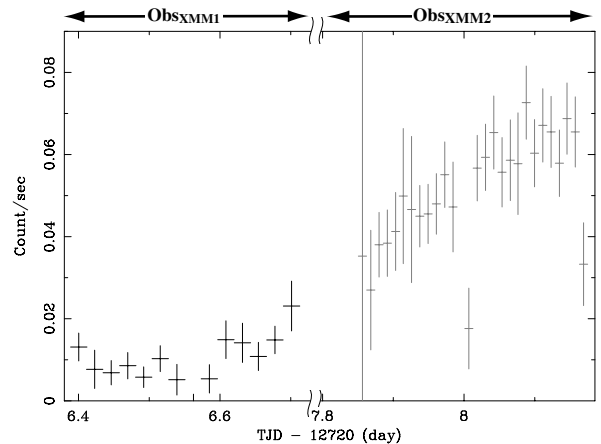


Figure 4. Light curve of IRS7B in the 2–10 keV band (EPIC pn plus MOS (1+2)) during the XMM-Newton observations. The horizontal axis is truncated Julian day (TJD) – 12720. Bins have 2 ksec for Obs<sub>XMM1</sub> and 1 ksec for Obs<sub>XMM2</sub>.

level by a linear increase. The time-scale of  $\sim 30$  ksec in Obs<sub>XMM2</sub> is much faster than the typical rising time-scale of solar-type X-ray flares of ksec, while X-ray flux in Obs<sub>XMM1</sub>, which is still a factor of  $\sim 10$  higher than those of the *Chandra* observation, was unchanged. Another fact is that, during both observations, the hardness ratio defined as count rates in the 5–10 keV band over those in the 2–5 keV band remained unchanged.

## 2.3. Spectra

Since the hardness ratio did not change significantly during each XMM-Newton observation, we extracted the spectra of IRS7B during the Obs<sub>XMM1</sub> and Obs<sub>XMM2</sub>.

The EPIC spectra of IRS7B in Obs<sub>XMM1</sub> and Obs<sub>XMM2</sub> (Figure 5) show several similarities: significant emission up to  $\sim 10$  keV; strong absorption below 2–3 keV; a broad line feature between 6–7 keV; marginal lines

between 5–6 keV in the EPIC pn spectra (which may be of instrumental or cosmic origin). To investigate the 6–7 keV line feature, we fit the EPIC pn and MOS (1+2) spectra simultaneously with an absorbed power-law model with a Gaussian component. An acceptable fit above 90% confidence has a photon index of 3.0 (2.5–3.4), a Gaussian line centroid of 6.60 (6.53–6.67) keV, and a Gaussian width of 0.15 (0.079–0.28) keV, where the numbers in parentheses denote the 90% confidence range. The derived Gaussian width, equivalent to  $\Delta v \sim 7,000$  km s<sup>-1</sup> if produced by Doppler broadening, is unreasonably large for a stellar plasma. We therefore interpret the broad feature as a blend of iron lines from a hot plasma at 6.7 keV and a fluorescent iron line at 6.4 keV though the profile needs to be confirmed with deeper observations.

The soft emission below 3 keV was unchanged between Obs<sub>XMM1</sub> and Obs<sub>XMM2</sub>, suggesting an additional component along with the hard emission. We therefore fit the spectra of Obs<sub>XMM1</sub> and Obs<sub>XMM2</sub> simultaneously with an absorbed 2T model — 1T for the variable hard component and 1T for the constant soft component — with a Gaussian line at 6.4 keV. In this model, we tied the  $N_{\text{H}}$  of the hard components in Obs<sub>XMM1</sub> and Obs<sub>XMM2</sub> and tied the elemental abundances of all components. We allowed  $N_{\text{H}}$  of the soft and hard components to be fit independently because a model fit with a common  $N_{\text{H}}$  gives large  $N_{\text{H}} \sim 2.4 \times 10^{23}$  cm<sup>-2</sup> and hence an unrealistically large intrinsic log  $L_X \sim 35$  ergs s<sup>-1</sup> for the soft component. The model successfully reproduced the spectra above the 90% confidence level. The derived physical parameters of the hard component are at the higher end among those of Class I protostars (e.g., see Imanishi et al., 2001, for comparison): large  $N_{\text{H}} \sim 2.8 \times 10^{23}$  cm<sup>-2</sup>, equivalent to  $A_V \sim 180^m$  (using the  $N_{\text{H}} - A_V$  relation by Imanishi et al. (2001)); plasma temperature of 3–4 keV; log  $L_X \sim 30.8$  ergs s<sup>-1</sup> in Obs<sub>XMM1</sub>, which further increased to  $\sim 31.2$  ergs s<sup>-1</sup> in Obs<sub>XMM2</sub>; and a fluorescent iron line equivalent width (EW) of  $\sim 810$  (240–1400) eV in Obs<sub>XMM1</sub> and  $\sim 250$  (100–400) eV in Obs<sub>XMM2</sub>. Meanwhile, the metal abundance is  $\sim 0.2$  (0.1–0.3) solar, which is typical of low-mass young stars (e.g. Favata et al., 2003).

### 3. DISCUSSION

We discovered an extremely embedded X-ray source at the position of the strong VLA centimeter radio source IRS7B in the IRS 7 star forming core. Thanks to its vicinity to the Sun ( $d \sim 170$  pc), the large effective area of *XMM-Newton* and an opportunity to catch an active phase, we obtained around  $\sim 2,000$  photons from IRS7B, which is about 40 times better than other extremely embedded X-ray sources observed so far. We discuss the mechanism to explain the observed X-ray properties.

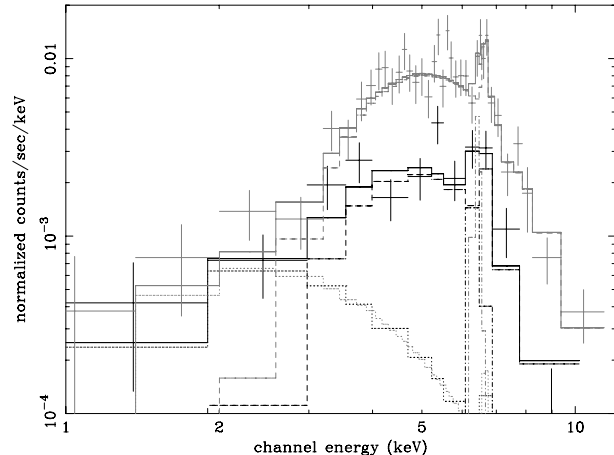


Figure 5. EPIC pn spectra of IRS7B in Obs<sub>XMM1</sub> (black) and Obs<sub>XMM2</sub> (gray). The solid lines show the best-fit model of the simultaneous fitting with EPIC pn and MOS. Dotted lines show the soft component, barred line the hard component, and dot-bar lines the Gaussian component for the line at 6.4 keV.

#### 3.1. What made the X-ray activity enhanced during the *XMM-Newton* observations?

Between the *Chandra* and *XMM-Newton* observations, IRS7B exhibited strong long-term X-ray variation by a factor of 10–100 on a timescale of a month (Figure 3). In none of the observations did we detect obvious flare activity though Obs<sub>XMM2</sub> showed a marked flux increase. Active stars such as RS CVn and young stars in open clusters do not generally vary in X-rays more than a factor of 2–3 outside flares (Stern, 1998). Less active stars such as the Sun exhibit strong X-ray variations by up to a factor of 100, coincident with their activity cycles (e.g. Favata et al., 2004), but, unlike IRS7B, the X-ray luminosity of such stars is typically less than  $10^{28}$  ergs s<sup>-1</sup> and the observed activity time scale is several years. One possibility is that the strong variability of IRS7B could indicate abrupt activity produced by an enhanced mass accretion episode similar to that recently attributed to the outburst of the star in McNeil’s nebula (Kastner et al., 2004). Indeed, the outburst increased the X-ray flux by a factor of 50, and the post-outburst X-ray luminosity of  $10^{31}$  ergs s<sup>-1</sup> is comparable to the luminosity of IRS7B during Obs<sub>XMM2</sub>.

The plasma temperature and X-ray luminosity of IRS7B during the *XMM-Newton* observations exceed the typical quiescent X-ray activity of Class I protostars and are comparable to temperatures and luminosities of X-ray flares from Class I protostars (Imanishi et al., 2001; Shibata & Yokoyama, 2002)<sup>1</sup>. X-ray flares from Class I protostars may be produced by reconnection in a magneto-

<sup>1</sup>Imanishi et al. (2001) used the distance to the  $\rho$  Oph cloud of 165 pc instead of 120 pc derived from more reliable *HIPPARCOS* data (Knupe & Høgg, 1998) for a comparison to earlier X-ray results of the  $\rho$  Oph field. Their X-ray luminosity should be divided by a factor of two to compare to our result.

sphere which is twisted due to the core-disk differential rotation (Tsuboi et al., 2000; Montmerle et al., 2000).

Perhaps mass accretion outburst during the *XMM-Newton* observations, accompanied with the magnetic activity similar to those of Class I protostars, explains the X-ray emission from IRS7B, though magnetic reconnection would have to occur throughout the *XMM-Newton* observations since no rapid X-ray variation was seen from IRS7B.

### 3.2. How is the X-ray Time Variation made during the *XMM-Newton* Observations?

If the fluorescent iron line in the spectra is real, this is unusual because fluorescent iron lines have been rarely observed from pre-main-sequence stars. Even a few examples during strong flares from Class I protostars have  $\text{EW} \lesssim 150$  eV (Imanishi et al., 2001). The large equivalent width of the fluorescent line from IRS7B ( $\sim 250\text{--}800$  eV) again suggests that the source is extremely embedded. When we simulate fluorescent iron line EWs, assuming solar abundance for the surrounding cold gas (Inoue, 1985), an optically thick absorber should block the direct X-ray emission by  $\sim 60\%$  for  $\text{Obs}_{\text{XMM1}}$  and  $\sim 3\%$  for  $\text{Obs}_{\text{XMM2}}$ . This result is consistent with obscuration of the X-ray emission though the blocking factor in  $\text{Obs}_{\text{XMM2}}$  should be  $\gtrsim 30\%$  to explain the observed flux increase in  $\text{Obs}_{\text{XMM2}}$ . Interestingly, the intrinsic X-ray luminosity in  $\text{Obs}_{\text{XMM1}}$  should be  $\log L_X \sim 31.2$  ergs  $\text{s}^{-1}$ , which is comparable to  $L_X$  in  $\text{Obs}_{\text{XMM2}}$ .

The flux increase of a factor of two in  $\sim 30$  ksec in  $\text{Obs}_{\text{XMM2}}$  is unlike the types of variations seen in magnetically driven X-ray flares which are characterized by rapid ( $\sim 10$  ksec) flux increases (e.g. Tsuboi et al., 1998, 2000; Stelzer et al., 2000; Imanishi et al., 2001). Favata et al. (2003) found a similar rise in X-ray brightness in the classical T-Tauri star XZ Tau, with a factor of 4 increase during 50 ksec. In this case, the brightening was accompanied by an  $N_{\text{H}}$  decrease and therefore Favata et al. (2003) interpreted it as an eclipse of the emitting region by the accretion stream. Because IRS7B did not show any significant hardness ratio variation the absorber would have to be uniformly dense, optically thick gas. Such a variation could be produced by an eclipse of the X-ray emitting region by an absorber or emergence of the X-ray emitting region from behind the rim of the protostellar core as a result of stellar rotation. To be consistent with the observed *XMM-Newton* light curves, the rotational period of the proto-stellar core would need to be  $\gtrsim 2.8$  days. This rotation speed is much slower than the break-up rotation speculated for Class 0 protostars from rotational periods of Class I protostars (e.g. Montmerle et al., 2000).

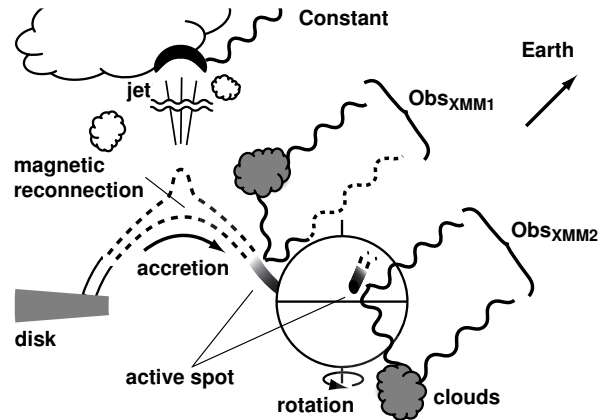


Figure 6. Possible picture of the structure around IRS7B.

### 3.3. What is the Constant Component below 3 keV?

The soft component was apparently constant and had much smaller  $N_{\text{H}}$  compared to the hard component. This may suggest that the component has no physical connection to, and exists far from, the hot component. One possible origin is that the soft component is associated with another hidden protostar, but, though the  $N_{\text{H}}$  of the soft component is typical of Class I protostars, the  $K$ -band magnitude of  $\gtrsim 19^m$  is much larger than those of Class I protostars in the R CrA cloud ( $K \lesssim 11^m$ ). Another possible origin is that the X-ray plasma is heated by a collision of a steady jet or outflow from IRS7B with circumstellar gas, a mechanism thought to be associated with X-ray emission from HH2, L1551 IRS 5, and OMC 2/3 (Pravdo et al., 2001; Favata et al., 2003; Tsujimoto et al., 2004). Indeed, IRS7B is associated with a centimeter radio source as those systems are, but the plasma temperature and X-ray luminosity of IRS7B are very large compared to those sources, except for the source in OMC 2/3. Such a high plasma temperature requires an energetic jet with  $v_{\text{jet}} \sim 1,500$  km  $\text{s}^{-1}$ . While low-mass young stars generally have slow outflow velocities (a few hundred km  $\text{s}^{-1}$ ), Marti et al. (1995) measured a large proper motion in the young stellar jets HH80-81 implying velocities up to 1,400 km  $\text{s}^{-1}$ . IRS7B could be another example of a source with high speed outflow.

## 4. A POSSIBLE PICTURE AROUND IRS7B

Figure 6 illustrates a possible picture of the X-ray emission mechanism and the structure around IRS7B. During a mass accretion outburst, high energy particles accelerated by the magnetic activity between the stellar core and circumstellar disk hit the stellar surface to produce hot plasma of  $kT \sim 4$  keV. The X-ray emission from the plasma is partly blocked when the spot would have been behind the protostar core during  $\text{Obs}_{\text{XMM1}}$ , and just ap-

peared from behind the rim in Obs<sub>XMM2</sub> as a consequence of protostellar rotation. The intensity of the fluorescent iron line did not change, but its EW decreases in Obs<sub>XMM2</sub> since the continuum emission from the hot plasma apparently increases. Jets ejected during the mass accretion activity in the past collide with circumstellar gas and emit constant X-rays.

## REFERENCES

- Anderson, I. M., Harju, J., Knee, L. B. G., & Haikala, L. K. 1997, *A&A*, 321, 575
- André, P., Ward-Thompson, D., & Barsony, M. 1993, *ApJ*, 406, 122
- Brown, A. 1987, *ApJ*, 322, L31
- Chini, R., Kämpgen, K., Reipurth, B., Albrecht, M., Kreysa, E., Lemke, R., Nielbock, M., Reichertz, L. A., Sievers, A., & Zylka, R. 2003, *A&A*, 409, 235
- Choi, M., & Tatematsu, K. 2004, *ApJ*, 600, L55
- Favata, F., Giardino, G., Micela, G., Sciortino, S., & Damiani, F. 2003, *A&A*, 403, 187
- Favata, F., Micela, G., Baliunas, S. L., Schmitt, J. H. M. M., Güdel, M., Harnden, F. R., Sciortino, S., & Stern, R. A. 2004, *A&A*, 418, L13
- Feigelson, E. D., Carkner, L., & Wilking, B. A. 1998, *ApJ*, 494, L215
- Grosso, N., Montmerle, T., Feigelson, E. D., André, P., Casanova, S., & Gregorio-Hetem, J. 1997, *Nature*, 387, 56
- Hamaguchi, K., Corcoran, M. F., Petre, R., White, N. E., Stelzer, B., Nedachi, K., Kobayashi, N., & Tokunaga, A. T. 2005, *ApJ*, 623, 291
- Harju, J., Haikala, L. K., Mattila, K., Mauersberger, R., Booth, R. S., & Nordh, H. L. 1993, *A&A*, 278, 569
- Harju, J., Higdon, J. L., Lehtinen, K., & Juvela, M. 2001, in *ASP Conf. Ser. 235: Science with the Atacama Large Millimeter Array*, ed. A. Wootten, p. 125–129
- Henning, T., Launhardt, R., Steinacker, J., & Thamm, E. 1994, *A&A*, 291, 546
- Imanishi, K., Koyama, K., & Tsuboi, Y. 2001, *ApJ*, 557, 747
- Inoue, H. 1985, *Space Science Reviews*, 40, 317
- Kastner, J. H., Richmond, M., Grosso, N., Weintraub, D. A., Simon, T., Frank, A., Hamaguchi, K., Ozawa, H., & Henden, A. 2004, *Nature*, 430, 429
- Knude, J., & Høg, E. 1998, *A&A*, 338, 897
- Koyama, K., Hamaguchi, K., Ueno, S., Kobayashi, N., & Feigelson, E. D. 1996, *PASJ*, 48, L87
- Marti, J., Rodriguez, L. F., & Reipurth, B. 1995, *ApJ*, 449, 184
- Mewe, R., Kaastra, J. S., & Liedahl, D. A. 1995, *Legacy*, 6, 16
- Montmerle, T. 2005, in *Star Formation in the Era of Three Great Observatories*
- Montmerle, T., Grosso, N., Tsuboi, Y., & Koyama, K. 2000, *ApJ*, 532, 1097
- Morrison, R., & McCammon, D. 1983, *ApJ*, 270, 119
- Nutter, D. J., Ward-Thompson, D., & André, P. 2005, *MNRAS*, 357, 975
- Pontoppidan, K. M., Fraser, H. J., Dartois, E., Thi, W.-F., van Dishoeck, E. F., Boogert, A. C. A., d’Hendecourt, L., Tielens, A. G. G. M., & Bisschop, S. E. 2003, *A&A*, 408, 981
- Pravdo, S. H., Feigelson, E. D., Garmire, G., Maeda, Y., Tsuboi, Y., & Bally, J. 2001, *Nature*, 413, 708
- Rho, J., Ramírez, S. V., Corcoran, M. F., Hamaguchi, K., & Lefloch, B. 2004, *ApJ*, 607, 904
- Saraceno, P., André, P., Ceccarelli, C., Griffin, M., & Molinari, S. 1996, *A&A*, 309, 827
- Shibata, K., & Yokoyama, T. 2002, *ApJ*, 577, 422
- Skinner, S., Gagné, M., & Belzer, E. 2003, *ApJ*, 598, 375
- Stelzer, B., Neuhäuser, R., & Hambaryan, V. 2000, *A&A*, 356, 949
- Stern, R. A. 1998, in *ASP Conf. Ser. 154: Cool Stars, Stellar Systems, and the Sun*, 223–+
- Tsuboi, Y., Imanishi, K., Koyama, K., Grosso, N., & Montmerle, T. 2000, *ApJ*, 532, 1089
- Tsuboi, Y., Koyama, K., Hamaguchi, K., Tatematsu, K., Sekimoto, Y., Bally, J., & Reipurth, B. 2001, *ApJ*, 554, 734
- Tsuboi, Y., Koyama, K., Murakami, H., Hayashi, M., Skinner, S., & Ueno, S. 1998, *ApJ*, 503, 894
- Tsujimoto, M., Koyama, K., Kobayashi, N., Saito, M., Tsuboi, Y., & Chandler, C. J. 2004, *PASJ*, 56, 341
- van den Ancker, M. E. 1999, PhD thesis, Universiteit van Amsterdam
- Wilking, B. A., McCaughrean, M. J., Burton, M. G., Giblin, T., Rayner, J. T., & Zinnecker, H. 1997, *AJ*, 114, 2029